Distributed UAV-SAR: System Concept Overview and Error Model

1st Lamberti Lucas
Microwaves and Radar Institute
German Aerospace Center (DLR)
Weßling, Germany
lucas.lamberti@dlr.de

2nd Baumgartner Stefan
Microwaves and Radar Institute
German Aerospace Center (DLR)
Weßling, Germany
stefan.baumgartner@dlr.de

3rd Krieger Gerhard
Microwaves and Radar Institute
German Aerospace Center (DLR)
Weßling, Germany
gerhard.krieger@dlr.de

***Abstract*—Technological advances have opened up the possibility to combine small unmanned aerial vehicles (UAV) and radar sensors. In this paper, a novel, multistatic system concept is presented that incorporates several identical, fully digital, multichannel radar sensors carried by UAV platforms. Each single radar is implemented in a direct sampling architecture on an AMD Zynq Ultrascale+ RF System on Chip (RFSoC), and all processing steps are performed in the digital domain, offering a high level of flexibility to the system. The system is currently being build up and intended primarily to serve as a research and development platform for the exploration of new multistatic synthetic aperture radar (SAR) imaging modes and techniques such as single-pass tomography, multi-baseline interferometry and holography, as well as new acquisition modes and techniques for future NewSpace SAR missions. Due to the individual local oscillators in each radar unit, accurate time, frequency and phase synchronisation is crucial for achieving a good multistatic measurement and imaging performance. An error model as well as the results of first ground-based experiments will be presented for mono- and multistatic measurements with the digital radars.**

***Index Terms*—synthetic aperture radar, multistatic, synchronization**

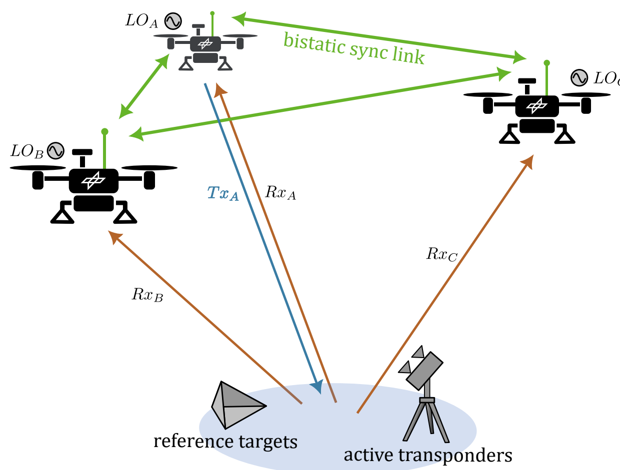

Fig. 1. Example visualisation of the multistatic radar system

I. Introduction

Synthetic aperture radar (SAR) imaging has become an established technique to gain unique information for applications such as climate change research, earth monitoring, ship detection, environmental research, forestry and agriculture as well as security related applications [1]. In multistatic SAR systems, the transmitter and receiver units are not located on the same platform and are typically separated by a considerable distance [2], offering several benefits. Single-pass multi-baseline cross- or along-track interferometry as well as tomographic and holographic imaging SAR can be accomplished with several baselines, without the negative impact of temporal decorrelation, which is a major drawback of repeat-pass observations [3], [4]. Due to technological advances in recent years, multistatic unmanned aerial vehicle (UAV) based radar systems have become a new field of interest, offering higher flexibility, lower development costs, and a faster deployment time [5]. New multistatic SAR concepts can be explored more rapidly, providing a valuable building block towards NewSpace SAR [6], [7].

Although several investigations have been carried out with monostatic UAV-based SAR [3], [8]–[11], not much can be found about multistatic UAV-SAR in open literature [4].

A novel distributed UAV-based SAR system is currently being built at the German Aerospace Center (DLR). The radar sensors are developed as fully digital, multichannel, direct radio frequency (RF) sampling sensors on an AMD Zynq Ultrascale+ RF System on Chip (RFSoC). Since the core components of the radar system are implemented on the field programmable gate array (FPGA) of the RFSoC, it offers a high reconfigurability and can be reprogrammed to investigate different, novel radar concepts and techniques. The UAV fleet (cf. Fig. 1) shall work in several synchronous and coherent acquisition modes. For instance, MirrorSAR [12], multistatic SAR, multiple-input multiple-output (MIMO), and other novel acquisition schemes. As the system can be used as a whole or with only a subset of its radar units and UAVs, it provides a broad field of applications such as environmental or traffic monitoring, infrastructure monitoring, disaster management, coastal protection and maritime security as well as agriculture, forestry and archaeology.

II. Multistatic System Concept

Since each radar will have its own local master oscillator (cf. Fig. 1), synchronisation errors in time, frequency, and phase are unavoidable and have to be compensated [13], [14]. Contrary to monostatic systems, oscillator noise does not cancel out in the multistatic case and can lead to several unwanted effects like additional range shifts, increased and unbalanced sidelobes, and a loss of resolution [14], [15]. Since internal logic counters are driven by the individually free running local master clocks, the local timestamps for transmission and reception on each radar unit will vary and drift apart over time [4]. Different synchronisation concepts have been developed in past years. A dedicated, bidirectional synchronisation channel (cf. green arrow in Fig. 1) will serve to test and implement several such methods, incorporating the exchange of different types of reference signals [4], [16]–[18] or new transponder based multistatic methods as presented in [12], [19], [20]. Additionally, ground reference targets and active transponders can be used to further improve the synchronisation.

Furthermore, the UAV platforms will not be able to follow the desired ideal flight paths exactly and will suffer from trajectory disturbances. This results in varying baselines between the UAVs so that motion compensation has to be considered during SAR processing. A custom-made localisation unit with an accurate multichannel and multiband global naviagion satellite system (GNSS) real time kinematic (RTK) receiver and an innertial measurement unit (IMU) will be integrated onto each UAV platform, providing precise position, orientation, and absolute time measurements (Fig. cf. 2).

III. Radar Sensors and Localisation Units

Each UAV-borne digital radar unit is intended to fly in user defined formations with a maximum altitude of 120 m above ground level (AGL). The system is designed to collect a scene size of 1 km^2, which will lead to long acquisition times of about 30 min when a velocity of 10 $\mathrm{m/s}$ is assumed. A block diagram of a single UAV payload is shown in Fig. 2. Each radar unit will have up to four transmit and four receive antennas, enabling transmission and reception in both horizontal and vertical polarisation. At the core of each digital radar unit is the RFSoC board (Fig. 2 left), which houses, among others, the digital to analog converters (DACs) and analog to digital converters (ADCs) that sample the signals directly in the RF domain. The radar unit will be tightly integrated with a localisation unit (Fig. 2 right), providing RTK measurements with GNSS based coordinated universal time (UTC) timestamps. The absolute position accuracy will be in the order of $\leq$1 cm and orientation angle accuracy $\leq$0.25 °. Since the radar is fully digital, different radar waveforms such as linear frequency modulated (LFM), stepped frequency modulated (SFM) or other waveforms can be generated and transmitted. Additionally, parts of the radar processing such as mixing and deramping will be carried out in the digital domain on the RFSoC board.

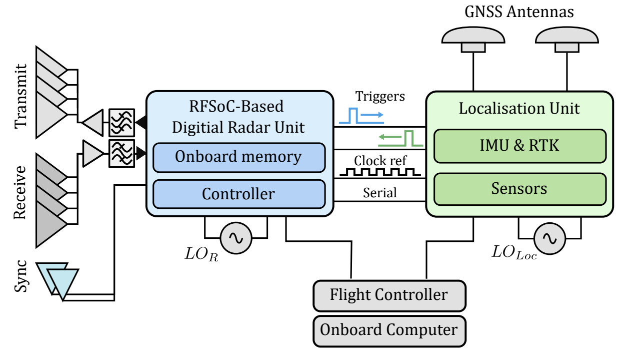

Fig. 2. Block diagram of a single UAV payload, showing the main system components.

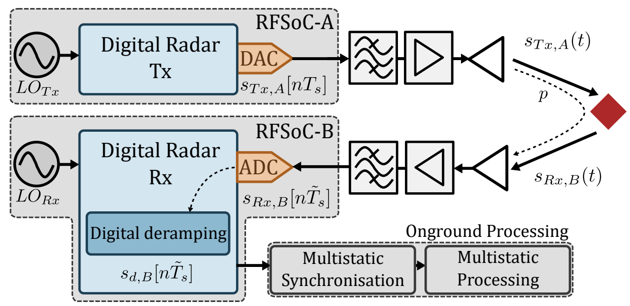

Fig. 3. Multistatic transmit and receive architecture. Example echo model for a point scatterer (red diamond).

IV. Challenges and Error Model

Each digital radar is driven by its own master local oscillator (LO). Different synchronisation errors arise that have to be compensated for multistatic processing. Those errors can be summarised into the following main problems [4], [14], [17], [21]:

- Clock drift of the local LOs, leading to timing and frequency errors, as well as sampling frequency errors.
- Uncompensated phase noise in the multistatic acquisitions, which will reflect itself in terms of sampling frequency jitter.
- Initial phase offsets and time offsets
- Different onboard latencies and path delays due to manufacturing tolerances.

For the setup shown in Fig. 3 a first frequency modulated continuous wave (FMCW) signal model incorporating all expected synchronisation errors is presented in the following. Transmitter and receiver are each on their separate RFSoC boards (a single one is shown in Fig. 4). The transmitted waveform at the transmitter antenna (cf. RFSoC-A in Fig. 3) can be described as:

$$s_{Tx,A}(t) = s_{ideal}(t) = e^{j2\pi\left(f_0 t + \frac{\alpha}{2} t^2\right)} \tag{1}$$

with the starting frequency f_0 and frequency ramp rate $\alpha = B/T_c$ being the ratio between modulation bandwidth B and chirp duration T_c. The echo received at the multistatic receiver RFSoC-B is directly sampled by the ADC. Deramping is done

Fig. 4. RFSoC board used in the radar sensors.

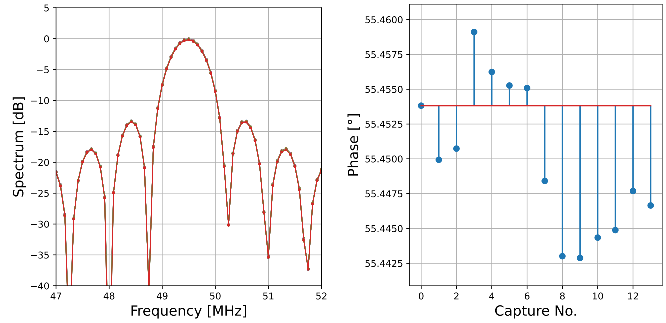

(a) (b)

Fig. 5. First monostatic, loopback measurements. a) Spectra of the deramped beat signals (overlayed), b) Phases at the peaks of the deramped beatsignals spectra.

in the digital domain with the ideally stored reference chirp samples. Synchronisation errors therefore occur at the domain crossings from the digital to the analog domain and vice versa. In a multistatic receiver (cf. RFSoC-B in Fig. 3), the received and sampled echo can show a deviating start frequency f_0', deviating chirp rate α' [17] and a deviating sampling interval $\tilde{T}_s = T_s(1+\epsilon)$. Moreover, the phase noise in the receiving LO causes jitter Δt_{jitt} in the ADC [21]. After the multistatic path delay $p = r/c$, with r being the travelled distance and c the speed of light, for a static point scatterer (cf. Fig. 3 right), the sampled signal by the receiver ADC is modelled as [22]:

$$s_{Rx,B}[n\tilde{T}_s] = e^{j2\pi\left(f_0'[n\tilde{T}_s - p + \Delta t_{jitt}] + \frac{\alpha'}{2}\left[n\tilde{T}_s - p + \Delta t_{jitt}\right]^2\right)} \quad (2)$$

Here $n = 0, 1, \ldots, N-1$ denotes the sample index and N the number of samples in the chirp. Due to time synchronisation offsets from different initial clocks and additional drift over time, the deramping reference will be shifted in time, which is expressed as a time delay Δt in the reference chirp:

$$s_{ref,B}[nT_s] = e^{j2\pi\left(f_0\cdot[nT_s - \Delta t] + \frac{\alpha}{2}[nT_s - \Delta t]^2\right)} \quad (3)$$

For deramping, (2) and (3) are conjugate multiplied to obtain the beatsignal:

$$\begin{aligned} s_{d,B}[n] =& s^*_{Rx,B}[n] \times s_{ref,B}[n] \\ & e^{j2\pi\left(\alpha' p\tilde{T}_s + \Delta\tilde{f}_0 - \alpha T_s \Delta t\right)n} \times \\ & e^{j2\pi\left(f_0' p - \frac{\alpha'}{2}p^2\right)} \times \\ & e^{j2\pi\left(\frac{\Delta\tilde{\alpha}}{2}n^2 - f_0\Delta t + \frac{\alpha}{2}\Delta t^2\right)} \times \\ & e^{j2\pi\phi[n\tilde{T}_s]} \end{aligned} \quad (4)$$

where $(\cdot)^*$ denotes complex conjugation, $\Delta\tilde{f}_0 = f_0 T_s - f_0'\tilde{T}_s$ and $\Delta\tilde{\alpha} = \alpha T_s^2 - \alpha'\tilde{T}_s^2$. The last term in (4) represents the phase noise terms, expressed as jitter Δt_{jitt} in the receiver ADC [21].

The error model is currently further developed to simulate all relevant occurring multistatic synchronisation errors and their effects on SAR imaging. It will serve as a base to develop and investigate different synchronisation methods for the multistatic radars.

V. First Simulation and Measurement Results

The digital radar system is still under development. First experiments have been done using a DAC and ADC channel on the same RFSoC board to transmit and receive linear FMCW chirps via a loopback cable in a monostatic arrangement (cf. Fig. 4). Over a timespan of 140 min, 14 chirps have been transmitted and collected. The chirp is generated in the software system of the board via C++ code and stored in the internal random access memory (RAM) of the Zynq processor. It is then transmitted to the DAC while simultaneously samples incoming from the ADC are written to another memory region. Deramping is performed offline with the ideal reference chirp and a subsequent fast Fourier transform (FFT) yields a peak at the frequency according to the time delay through the system and the loopback cable (Fig. 5a). The oscillator built into the RFSoC board is a oven-controlled crystal oscillator (OCXO) by Connor Winfield with frequency tolerances in the order of ± 3 ppm s [23]. The phases at the peaks of Fig. 5a, shown in Fig. 5b, show a spread of about 0.016 $^\circ$ with a variance of $2.62{\times}10^{-}5$ $^\circ$, indicating good stability of the used LO for the monostatic receiver. However, internal time counters still need to be adjusted or tracked periodically, since time drifts in the order of $\approx$ 5.4 ms can occur in the worst case, over the planned long collection times of about 30 min.

Multistatic, cable bound measurements between two boards are currently performed. The results will be included in the final paper.

VI. Outlook and Preliminary Conclusions

First measurements with the RFSoC board have been developed and will be further extended. The first monostatic measurements suggest a good short-term stability and quality of the digitally generated chirps. This is currently further investigated for the reception with two independent RFSoC boards. Besides the timing offsets between two independent boards, phase noise of the LOs is expected. In anticipation, a first multistatic error model for the digital radar has been derived and will be further developed and verified with the multistatic measurements. These investigations and the obtained results will be shown in the final paper.

REFERENCES

[1] A. Moreira, P. Prats-Iraola, M. Younis, G. Krieger, I. Hajnsek, and K. P. Papathanassiou, "A tutorial on synthetic aperture radar," *IEEE Geoscience and Remote Sensing Magazine*, vol. 1, no. 1, pp. 6–43, 2013.

[2] G. Krieger and A. Moreira, "Spaceborne Bi- and Multistatic SAR: Potential and Challenges," *IEE Proceedings - Radar Sonar and Navigation*, vol. 153, pp. 184–198, 08 2013.

[3] V. Mustieles Pérez, S. Kim, C. Bonfert, G. Krieger, and M. Villano, "Towards UAV-Based Ultra-Wideband Multi-Baseline SAR Interferometry," in *20th European Radar Conference, EuRAD 2023*, 2023. [Online]. Available: https://elib.dlr.de/202949/

[4] Y. Wang, Z. Ding, L. Li, M. Liu, X. Ma, Y. Sun, T. Zeng, and T. Long, "First Demonstration of Single-Pass Distributed SAR Tomographic Imaging With a P-Band UAV SAR Prototype," *IEEE Transactions on Geoscience and Remote Sensing*, vol. 60, pp. 1–18, 2022.

[5] J. Kim, S. Kim, W. Lee, S. Shin, Y. Choi, and M.-H. Ka, "Design and Implemetation of Compact 77 GHz Synthetic Aperture Radar for Drone Based Applications," in *2019 6th Asia-Pacific Conference on Synthetic Aperture Radar (APSAR)*, 2019, pp. 1–5.

[6] M. Villano, M. N. Peixoto, S. Kim, V. M. Pérez, N. Ustalli, J. Mittermayer, T. Börner, G. Krieger, and A. Moreira, "Potential of Multi-Static SAR Systems for Earth Monitoring and Their Demonstration Using Swarms of Drones," in *IGARSS 2023 - 2023 IEEE International Geoscience and Remote Sensing Symposium*, 2023, pp. 4586–4589.

[7] M. Villano, M. Nogueira Peixoto, L. Dell'Amore, S.-Y. Jeon, N. Ustalli, J. Krecke, J. Mittermayer, G. Krieger, and A. Moreira, "NewSpace SAR: Disruptive Concepts for Cost-Effective SAR System Design," in *EUSAR 2021; 13th European Conference on Synthetic Aperture Radar*, 2021, pp. 1–6.

[8] S. Kim, V. M. Pérez, G. Krieger, and M. Villano, "Three-Dimensional Structure Inversion Through Wide Fractional Bandwidth, UAV-Based SAR Interferometry," in *2023 24th International Radar Symposium (IRS)*, 2023, pp. 1–10.

[9] S. Dill, A. Heinzel, M. Engel, and M. Peichl, "DRONAR – A drone-borne radar for the detection of landmines and booby traps," in *Wehrwissenschaftliche Forschung - Jahresbericht 2021*, ser. Wehrwissenschaftliche Forschung, U. A. I. BMVg, Ed., August 2022, vol. 2021, pp. 44–45. [Online]. Available: https://elib.dlr.de/193675/

[10] M. García Fernández, Y. Álvarez López, A. Arboleya Arboleya, B. González Valdés, Y. Rodríguez Vaqueiro, F. Las-Heras Andrés, and A. Pino García, "Synthetic Aperture Radar Imaging System for Landmine Detection Using a Ground Penetrating Radar on Board a Unmanned Aerial Vehicle," *IEEE Access*, vol. 6, pp. 45 100–45 112, 2018.

[11] R. Burr, M. Schartel, A. Grathwohl, W. Mayer, T. Walter, and C. Waldschmidt, "UAV-Borne FMCW InSAR for Focusing Buried Objects," *IEEE Geoscience and Remote Sensing Letters*, vol. 19, pp. 1–5, 2022.

[12] G. Krieger, M. Zonno, M. Rodriguez-Cassola, P. Lopez-Dekker, J. Mittermayer, M. Younis, S. Huber, M. Villano, F. Q. de Almeida, P. Prats-Iraola, and A. Moreira, "MirrorSAR: A fractionated space radar for bistatic, multistatic and high-resolution wide-swath SAR imaging," in *2017 IEEE International Geoscience and Remote Sensing Symposium (IGARSS)*, 2017, pp. 149–152.

[13] M. Weiss, "Synchronisation of bistatic radar systems," in *IGARSS 2004. 2004 IEEE International Geoscience and Remote Sensing Symposium*, vol. 3, 2004, pp. 1750–1753 vol.3.

[14] G. Krieger and M. Younis, "Impact of oscillator noise in bistatic and multistatic SAR," *IEEE Geoscience and Remote Sensing Letters*, vol. 3, no. 3, pp. 424–428, 2006.

[15] E. Loria, S. Prager, I. Seker, R. Ahmed, B. Hawkins, and M. Lavalle, "Modeling the Effects of Oscillator Phase Noise and Synchronization on Multistatic SAR Tomography," *IEEE Transactions on Geoscience and Remote Sensing*, vol. 61, pp. 1–12, 2023.

[16] H. Breit, M. Younis, U. Balss, A. Niedermeier, C. Grigorov, J. Hueso-Gonzalez, G. Krieger, M. Eineder, and T. Fritz, "Bistatic synchronization and processing of TanDEM-X data," in *2011 IEEE International Geoscience and Remote Sensing Symposium*, 2011, pp. 2424–2427.

[17] M. Stefko, O. Frey, C. Werner, and I. Hajnsek, "Calibration and Operation of a Bistatic Real-Aperture Polarimetric-Interferometric Ku-Band Radar," *IEEE Transactions on Geoscience and Remote Sensing*, vol. 60, pp. 1–19, 2022.

[18] M. Ash, M. Ritchie, K. Chetty, and P. Brennan, "A New Multistatic FMCW Radar Architecture by Over-the-Air Deramping," *IEEE Sensors*, 08 2015.

[19] N. Ustalli, G. Krieger, J. Mittermayer, M. Villano, and C. Waldschmidt, "MirrorSAR Concept: Phase Synchronization Analysis," in *2022 Kleinheubach Conference*, 2022, pp. 1–4.

[20] A. Grathwohl, B. Meinecke, M. Widmann, J. Kanz, and C. Waldschmidt, "UAV-Based Bistatic SAR-Imaging Using a Stationary Repeater," *IEEE Journal of Microwaves*, vol. 3, no. 2, pp. 625–634, 2023.

[21] C. Azeredo-Leme, "Clock Jitter Effects on Sampling: A Tutorial," *IEEE Circuits and Systems Magazine*, vol. 11, no. 3, pp. 26–37, 2011.

[22] C. J. Cochrane, K. B. Cooper, S. L. Durden, R. Rodriguez Monje, and R. J. Dengler, "An FPGA-Based Signal Processor for FMCW Doppler Radar and Spectroscopy," *IEEE Transactions on Geoscience and Remote Sensing*, vol. 58, no. 8, pp. 5552–5563, 2020.

[23] *Surface Mount Oven Stabilized Oscillator DOCSC01-Series*, Connor Winfield, 02 2024, rev. 03.